
# Effect of Varying Volume Concentration of Nanoparticles (CuO) In Light Water Nuclear Reactor on Heat Transfer

**Samah Jalil Mohsen[1],**

[1,2]University of Thi-Qar College of Engineering Mechanical Engineering Department
engnarjiseng@gmail.com

**Ahmed Jassem Shkarah[2]**

[1,2]University of Thi-Qar College of Engineering Mechanical Engineering Department

**Abstract**

Nanofluid is crucial for improving heat conduction in nuclear power plants. It opens up new opportunities for improving heat transfer and reducing thermal hydraulics problems in nuclear reactors. The purpose of this research is to quantitatively illustrate the heat transfer performance of a CuO/Water-based nanofluid in a light water nuclear reactor. The hexagonal form of the nuclear fuel rod assembly's 1/6th was used in this study's modelling. The thermal properties of conventional fluid are improved using CuO/water nanofluid. A constant heat flux is applied to the inner wall. The link between nanofluid flow rate and nanoparticle concentration is shown by profiles of the temperature near to the wall and the heat transfer coefficient.

The amount of heat that a nanofluid can transport may depend on its volume concentration, physical properties, and nanoparticle size. Density, thermal conductivity, specific heat, and viscosity were investigated and utilised as the fundamental data for ANSYS 19. In order to increase the precision of the findings, the k-SST turbulence model is investigated. Two volumes of concentration—1% and 2%—are used in this numerical study. Results are compared to mathematical formulae for heat transmission. The results show that a single phase model significantly improves predictions of heat transport in nanofluids. The Reynold Number enhances the heat transfer coefficient, according to the results. It also demonstrates that the temperature near the wall is dropping as a result of the nanoparticle addition.

**Keywords:** CFD, , Heat Transfer Coefficient, CuO/water nanofluid

## 1. Introduction

Currently, there is a significant increase in the demand for energy as a result of population expansion. The enhancement of efficiency in industrial sectors is heavily reliant on the optimisation of cooling processes. Cooling plays a significant part in mitigating thermal hydraulics issues in nuclear power production. Several typical fluids with low heat conductivity, such as water, oil, gases, and different refrigerants, have been used (Sharma, 2015:36).

In recent years, researchers have developed a novel approach to enhance heat transmission

by incorporating nano-sized metallic particles into a base fluid. The aforementioned approach exhibited drawbacks stemming from inadequate suspension stability and the generation of erosion inside channels. In 1995, the Argonne National Laboratory in the United States introduced the notion of nanofluids (Sharma & Pandey, 2016:16).

Over the course of previous decades, a considerable amount of experimental and numerical investigations have been conducted with the aim of improving the heat transfer characteristics of nanofluids. A limited number of experimental experiments have been conducted to assess the impact of particle size regarding the characteristics of heat transfer in laminar fluid flow (Hegde et al., 2014:1287).

An experiment was conducted using two distinct particle sizes: one with a diameter of 45 nm and the other with a diameter of 150 nm. The experimental examination revealed that both nanofluids exhibited a higher heat transfer coefficient compared to the base fluid. However, it was observed that the heat transfer coefficient was greater for particles with smaller diameters compared to those with larger diameters (Sharma & Pandey, 2017:112).

The current study conducted a numerical analysis on heat transmission in a circular tube using nanofluids. The findings of this inquiry indicate that an increase in particle size results in a drop in the heat transfer coefficient. Fotukian et al. (5) conducted an experimental study to investigate the pressure drop and heat transfer enhancement in turbulent flow inside a circular tube (Acir et al., 2021:79).

It has been discovered that there is a 20% decrease in pressure inside a circular tube as a result of a 25% increase in heat transmission. It was also noted that when the Reynold number climbed, there was an increase in the heat transmission coefficient, but the temperature next to the wall dropped. The study conducted by Fotukian et al. (2010) shown that the addition of a smaller quantity of Al2O3 nanoparticles to the base fluid, water, resulted in an increase in heat transfer (Rohini Priya et al., 2012:17).

However, the effect of varied concentrations of Al2O3 particles did not have a significant impact. The current study used a computational approach to examine the behaviour of CuO nanoparticles at low concentrations. The primary objective of this study is to examine the heat transfer properties of a CuO/Water nanofluid under turbulent flow conditions inside a 1/6th segment of a hexagonal fuel rod assembly (Haq & Aman, 2019:401).

## 2. Mathematical and Numerical Modelling

This numerical study focuses on the examination of VVER-440 type reactors. The assembly has 61 fuel rods placed in a hexagonal shape. The simulation employs a triangle structure consisting of 8 complete rods, 4 half rods, and a centre rod, placed in a triangular pattern. The whole vertical dimension of the fuel rod bundle is 1000 mm (Wang et al., 2019:187).

The pitch of the fuel rods is measured to be 12.75mm, while the inner and outer diameters of the rods are recorded as 9.1mm and 7.57mm, respectively. Figure (2,1) depicts a comprehensive representation of a rod bundle assembly, whereby a distinct triangular structure of the rod bundle is visually evident. The coolant is seen to exhibit axial flow inside the subchannel, which is situated between the rods (Elsebay et al., 2016:6439).

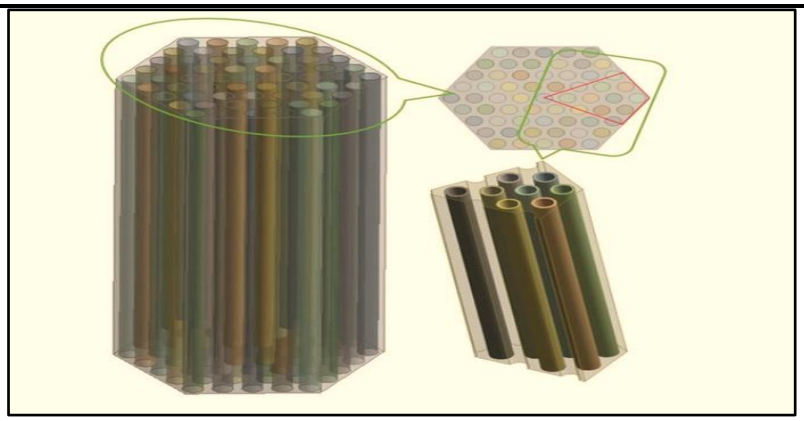

Figure (2,1): Geometry diagram under research. (Rowan & Seaid, 2020:474)

The composition of rods consists of uranium dioxide, whereas the top portion of the rod is constructed using a cladding material known as Zircaloy

### 2.1 Boundary Conditions and Simulation

In order to successfully carry out the numerical research, sufficient boundary conditions are essential. The nanofluid, which is utilised as a coolant in this numerical experiment, flows in the domain with a velocity of 3.5m/s and a temperature of 265 °C. At the intake, the turbulence intensity was set at 5%. The fuel rod bundle has a hydraulic diameter of 6.45 mm. The pressure of the nanofluid coolant assumed at the intake is 124 bar (Ernestová et al., 2007:188).

The boundary condition for triangle walls is no slip adiabatic, while the boundary condition to supply rod walls is no slip with a uniform heat flux of 1047340 W/m2. At the fuel rod bundle's outflow, the pressure is set to zero. The k- SST turbulence model was utilised in the current computational experiment to discretize the domain using the finite volume approach (Janosy et al., 2010:166)

The leading model for high convergence and accuracy in simulated results is k- SST because it can anticipate the flow in the wake of the sub channel extremely effectively. CFX is used to solve the governing equations used in this inquiry. For convective & diffusive parameters, the central difference method scheme and the QUICK scheme were used, respectively. Figures (2,2) illustrate the results of testing several meshes with varied element sizes (Khan et al., 2012:129). The convergence requirement was extremely well fulfilled, as seen in Table (2,1).

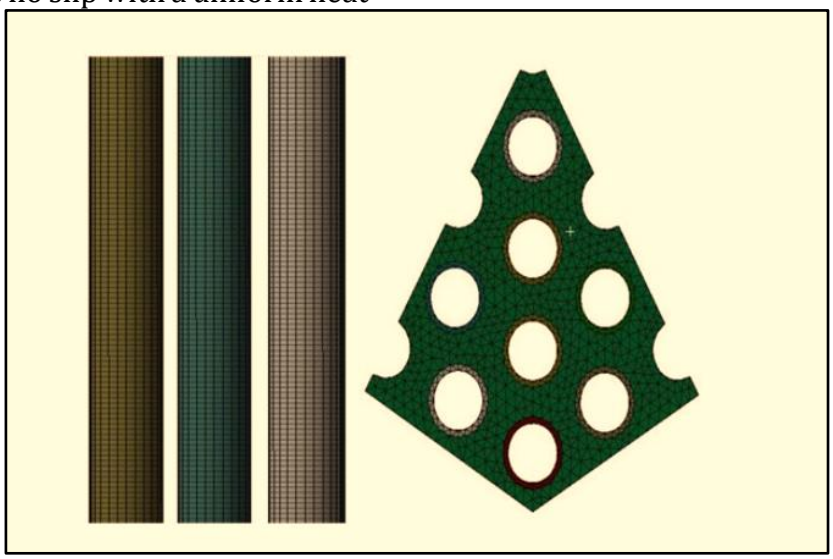

Figure (2,2): Geometric model meshing in multiple sectional views (Capson-Tojo et al., 2022:1158)

### 2.2 Sufficient boundary condition

In order to successfully carry out the numerical research, sufficient boundary conditions are required. The nanofluid is utilised as a coolant in this numerical experiment, flowing through the domain at a velocity of 3.5m/s and a temperature of 538k°. At the intake, the turbulence intensity was set at 5%. The hydraulic diameter of the fuel rod bundle is 6.45 mm (Gupta & Curtin, 2021:5658).

The intake assumes a 124 bar pressure for the nanofluid coolant. The boundary condition for triangle-shaped walls is no slip adiabatic, whereas the boundary condition for rod-shaped walls is no slip with two constant heat flux values (1000000 and 1055000) W/m2. The pressure is zero at the output of the fuel rod bundle. The present numerical experiment used the k-SST turbulence model to discretize the domain using the finite volume technique (Kubo et al., 2014:246).

## 3. Modelling and the Equations of Condition

These studies assume the following conditions, which are based on the single-phase model and the governing coefficients of steady fluid flow.

1. Fluid motion is incompressible, Newtonian, and turbulent by definition.
2. The nanoparticles and fluid are both at the same temperature.
3. We only take into account non-radiative effects and give little weight to vicious ones.

The three-dimensional models' continuity, momentum, and energy equations have been addressed under the aforementioned conditions. It is possible to express the Navier-Stokes equations for incompressible flow in Cartesian coordinates, as shown below (Ernestová et al., 2007:191).

The principle of conservation of mass :

$$\omega.(\mathrm{p}_{eff}\,\bar{V}) = 0 \quad \text{.....(3,1)}$$

The principle of conservation of mass of moment:

$$\omega.(\mathrm{p}_{eff}\,\bar{\bar{V}}\bar{V}) = -\omega\,\bar{P} + \mu_{eff}\,\omega^2\,\bar{\omega} - \mathrm{p}_{eff}\,\omega(\bar{\upsilon}'\bar{\upsilon}') \quad \text{.....(3,2)}$$

The principle of conservation of mass of energy :

$$\omega.(\mathrm{p}_{eff}\,C_{P.eff}\,\bar{\bar{V}}\bar{T}) = \omega.(\mathrm{k}_{eff} + k_t)\omega.\bar{T} \quad \text{.....(3,3)}$$

The addition of nanoparticles significantly alters the thermophysical properties of solutions, with various factors playing a crucial role in this modification. These factors encompass the type of material, size and shape of the nanoparticles, volume concentration of the suspended particles, and conductivity of the base fluid. Novel fluid compositions have been developed, exhibiting distinct thermophysical characteristics including density, thermal diffusivity, thermal conductivity, convective heat transfer, heat capacity, , and viscosity. A schematic representation of the various thermophysical characteristics of nanofluids may be seen in Figure 7. (Sharma, 2015:37).

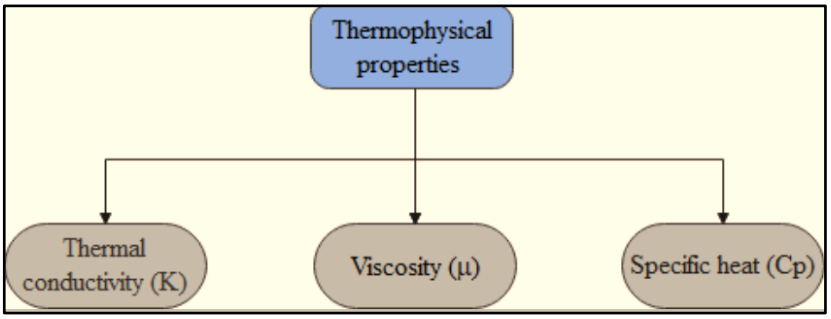


Figure (3, 1): The thermophysical characteristics of nanofluids.

## 4. Properties of Nanofluid

In order to evaluate the heat transfer characteristics, it is necessary to determine or estimate the properties of nanofluids, including density, specific heat, viscosity, and thermal conductivity. These parameters may be tested experimentally or predicted using theoretical models (Ernestová et al., 2007:194).

### 4.1 Thermal conductivity

Thermal conductivity refers to the intrinsic property of a substance that enables it to efficiently conduct or transport thermal energy.

Enhancing the thermal efficiency of a heat transfer fluid is mostly contingent upon its most crucial attribute. Numerous theoretical and experimental investigations were conducted to determine the thermal conductivity value of a nanofluid (Acir et al., 2021:81).

The dependence of this characteristic is contingent upon several factors, including the temperature of the medium, the conductivity of the base fluid, the thermophysical properties of the nanoparticles, the size and shape of the particles, the Brownian motion, as well as the volume fraction of the suspended particles (Haq & Aman, 2019:408).

Various techniques exist for measuring the thermal conductivity of nanofluids, including the transient hot-wire approach , the steady-state parallel plate method, the cylindrical cell method, the temperature oscillation method, and the 3w method. The work done by Esfe et al. (2016) investigated the thermal conductivity of Al2O3 nanoparticles dispersed in ethylene glycol (EG) over a range of volume concentrations, namely from 0.2% to 5.0%. The findings of this research indicate that there is a positive correlation between the concentration of nanoparticles and temperature with the effective thermal conductivity of Al2O3/EG nanofluids. The results showed a peak enhancement of 12.7% when the concentrations exceeded 1.0% (Rohini Priya et al., 2012:22).

### 3.2 Viscosity

The viscosity of fluids plays a crucial role in thermal applications. Furthermore, the process of heat transmission by convection is subject to the impact of viscosity. Due to its substantial influence on heat transmission, viscosity requires equal consideration to thermal conductivity. The primary factor contributing to the rise in viscosity of nanofluids is the augmentation of nanoparticle concentration, whereas the elevation of temperature leads to a reduction in viscosity (Acir et al., 2021:82).

A range of viscometers with different functional bases have been used for the purpose of quantifying the viscosity of nanofluids. These include the capillary tube viscometer, Vibroviscometer, rotating rheometer, drop/fall ball, piston viscometer, as well as cup viscometer. The most frequent types of instruments for determining the viscosity of nanofluids are the rotary rheometer, the piston rheometer, and the capillary tube viscometer, amongst others (Wang et al., 2019:189).

In their study, Moghaddam et al. (2019) synthesised nanofluids consisting of graphene and glycerol, and then conducted experimental investigations to evaluate the rheological characteristics of these nanofluids. The findings of this study suggest that the viscosity of nanofluids composed of graphene and glycerol is influenced by both the mass fraction and temperature variables. The viscosity is enhanced as the mass fraction increases and diminishes as the temperature increases (Ernestová et al., 2007:195).

The present study yielded a significant increase in the viscosity of glycerol, namely by 401.49%. This increase was achieved by incorporating 3% of graphene nanosheets into the glycerol matrix, while subjecting the mixture to a shear rate of 6.32 s−1 and maintaining a temperature of 20 °C. Einstein conducted research on the dynamic viscosity of a nanofluid, specifically focusing on a combination composed of sparse suspensions of small, spherical particles (Reinke et al., 2006:469). . The phrase that characterises this model may be stated as follows:

$$\mu_{nf} = \mu_f (1 + 2.5\varphi) \quad (3,4)$$

with *nf* representing the dynamic viscosity of the nanofluid and *f* being the dynamic viscosity of the base fluid, and with being the volume fraction of the nanoparticles.

### 3.3 Specific heat

Nanofluids' specific heat is a crucial property that significantly affects their thermal transfer rate. The amount of heat required to increase the temperature of 1g of nanofluid by 1C is its specific heat. Sang and Liu (2018) studied the specific improvement in heat capacity of ternary carbonate using four different nanoparticles (SiO2, TiO2, Al2O3, CuO).

In addition to demonstrating that the specific heat capacity of a nanofluid is highly dependent on the kind of nanoparticle and the nanostructure, their experimental results suggest that SiO2 nanoparticle is the best

particle to increase the specific heat capacities of ternary carbonate nanofluids. Researchers Sardinia et al. (2012) tested the specific thermal capabilities of CuO-based oil nanofluids at several temperatures, with particle weight fractions ranging from 0.2 to 2%. In this experiment, increasing concentrations of nanofluids resulted in a lower specific heat capacity compared to the base fluid (Haq & Aman, 2019:405).

This finding demonstrates that nanofluids, even at a concentration as low as 2% by weight, have a specific heat that is almost 23% lower compared to that of the base fluid at 40 °C. You may use any of these two equations to calculate the specific heat of a nanofluid (Wang et al., 2019:191).. Alternatively, according to Pak and Cho's estimates, the former is the case:

$$(\mathrm{C}_p)nf = (1-\alpha)(\mathrm{C}_p)_f + \alpha(C_P)\mathrm{s} \quad \text{.....(3,5)}$$

The specific temperatures of the nanofluid, base fluid, and nanoparticles are denoted as $(\mathrm{C}_p)nf$, $(\mathrm{C}_p)_f$, and $(C_P)\mathrm{s}$, respectively, which is the calculation of the effective density of the nanofluid is provided by Wang and Mujumdar which is as following:

$$\mathrm{C}_{p.nf} = \frac{(1-\alpha)\,\mathrm{p}_{bf}\mathrm{C}_{p.bf} + (\alpha)\,\mathrm{p}_{np}\mathrm{C}_{p.np}}{(1-\alpha)\,\mathrm{p}_{bf} + (\alpha)\,\mathrm{p}_{np}} \quad \text{.....(3,6)}$$

For the purpose of this research, the empirical correlation that Corcione proposed for nanofluid dynamics is utilised.

$$\frac{\mu_{nf}}{\mu_{bf}} = \frac{1}{1-34.87(d_{nb}/d_{bf})^{-0.3}\alpha^{1.08}} \quad \text{.....(3,7)}$$

where $d_{bf}$ is the base fluid's molecular equivalent diameter:

$$d_{bf} = 0.1\left\{\frac{6M}{N\pi}\right\}^{1/3} \quad \text{.....(3,8)}$$

Where N is the Avogadro constant, M the molecular weight of the base fluid, and $p_{bfo}$ the mass density of the base fluid at T=293 K. The effective thermal conductivity of a nanofluid was calculated as the following function of the nanofluid temperature, the mean diameter of the particles, the volume fraction of the nanofluid, the Reynolds number of the particles, and the thermal conductivity of the nanoparticles and the base fluid, using the Corcione correlation (Corcione, 2011:69).

$$\frac{k_{nf}}{k_{bf}} = 1 + 4.4\,\mathrm{Re}_{np}^{04}\,\mathrm{Pr}_{bf}^{0.66}\left\{\frac{T}{T_{fr}}\right\}^{10}\left\{\frac{k_{np}}{k_{bf}}\right\}^{0.03}\alpha^{0.66} \quad \text{.....(3,9)}$$

The $T_{fr}$ is the temperature at which the base fluid freezes (approximately 273.16 K). The Reynolds number of a nanoparticle is defined as:

$$\mathrm{Re}_{np} = \frac{2\,p_{bf}k_B T}{\pi\mu_{bf}^2 d_{np}} \quad \text{.....(3,10)}$$

Nanoparticles with a diameter of 10 nm to 150 nm, a concentration of 0.2% to 9% by volume, and a temperature of 294 K to 324 K are all within the range of this correlation (Wang et al., 2019:192).

### 3.4 Heat Transfer Analysis

Nanofluids' heat-transferring behaviour may benefit greatly from an improvement in effective thermal conductivity. But there are several more elements that have a role . Several other factors, such as the fluid's physical properties (such as its specific heat density, viscosity, average fluid velocity, etc.) or the geometry system (such as the tube's diameter and length), determine the coefficient for heat transfer in the absence of necessary convection. Therefore, direct heat transfer measurements of Nano fluids under appropriate flow conditions are required (Haq & Aman, 2019:412).. In this research, we assume that all the heat generated is cosine:

$$\mathrm{q}^n(y) = \frac{P}{4r_{in}l}\cos\left\{\frac{\pi y}{l}\right\} \quad \text{.....(3,11)}$$

P is the total power of the heater used in the test section, $r_{in}$ is the radius of the inner tube, and l = 1 m is the length of the heating area. Both the fluid temperature and the temperature of the wall opposite to which heat is being transferred must be known. The simulation helps get the target temperature next to the wall. Take an average of the temperatures on the left and right walls for an accurate reading (Reinke et al., 2006:470).

$$\mathrm{T}_{bulk} = \frac{T_{right} + T_{left}}{2} \quad \text{.....(3,12)}$$

The following equation (Incropera and DeWitt, 1996) may be used to get the bulk temperature:

$$\mathrm{T}_{bulk} = T_{in}\frac{q}{mc_p} \quad \text{.....(3,13)}$$

## 4. Validation

The analytical heat transport equation validates the numerical investigation's findings. A vertical triangular channel is used in numerical modelling to simulate flow through

nuclear fuel rods in a non-radiation situation . The analytical heat transport equation validates the numerical investigation's findings. According to Figure (2,2), the numerical modelling consists of a vertical triangular channel that is used to simulate flow through nuclear fuel rods in a non-radiation environment (Reinke et al., 2006:471).

When numerical results are compared to analytical results, the numerical results are more precise and superior. Figure (4,1) shows the wall-adjacent temperature profiles at Reynold number 10,000, and the 1% volume concentration is proven by analytical results. It is derived using a formula that is almost atop the result from ANSYS CFX (Haq & Aman, 2019:414).

$$T_m(Z) = T_{mi} + \left(\frac{q * p}{m * C_P}\right) Z \quad \text{.....(4,1)}$$

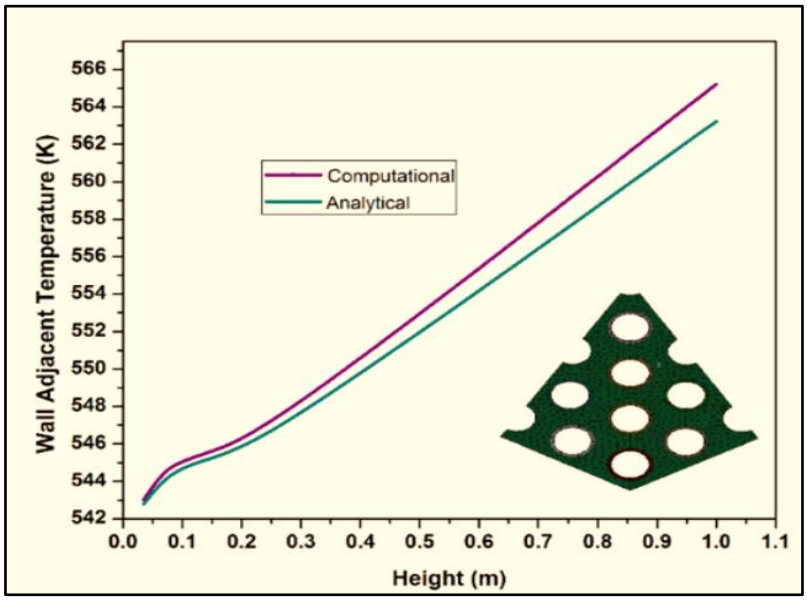


Figure (4,1): Analytical versus numerical temperature profile comparison.

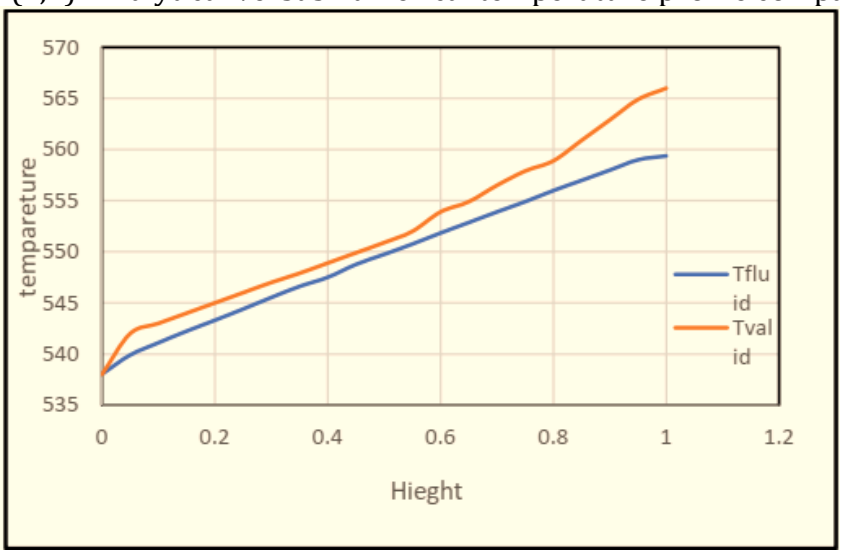


Figure (4,2):Acontrast between the analytical and numerical results of the temperature curve

## 5. Result and discussion

In this section, we give the findings of our numerical investigation of the vertical triangular channel. Here we report on the difference in heat transfer properties between no nanofluid and a nanofluid made of CuO and water. The contours of the walladjacent temperature of the clad, the heat transfer coefficient, and the velocity are shown in Figures (5,1), (5, 2), and (5,3).

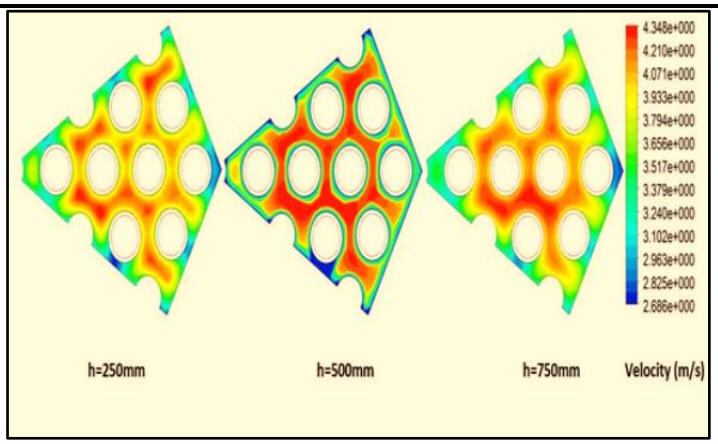


Figure (5,1): The velocity curve at the value of one ($\alpha$ =1)

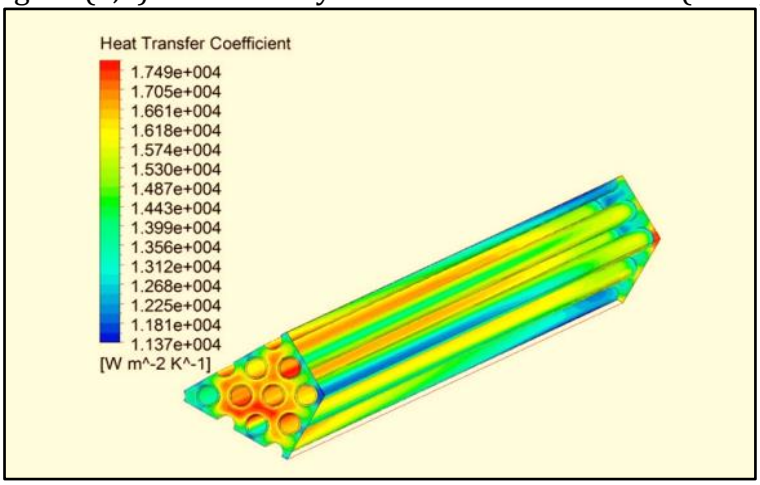


Figure (5,2): The Heat Transfer with Coefficient Equal to 1( $\alpha$ =1)

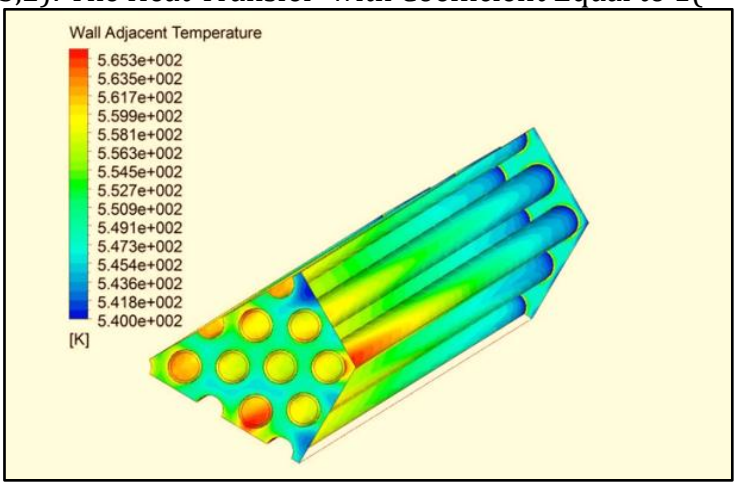


Figure (5,3): The Wall Adjacent Temperature at with Coefficient Equal to 1 ( $\alpha$ =1%)

In this part, we will do the calculations necessary for the vertical triangular channel's numerical study and then show our results. This section provides a report on the impact that using a nanofluid based on CuO and water has had on the heat transfer capabilities. Figures Figure (5,4) displays the contours of the wall adjacent temperature of the clad at a value of 1%. Figure (5,5) displays plots of the clad temperature for 1% nanofluid weight concentration at a variety of Reynolds numbers. As seen in Figure (5,5), the temperature of the clad wall decreases as the Reynold number increases. This is because the nanofluid's variable intake velocity causes the temperature to reduce.

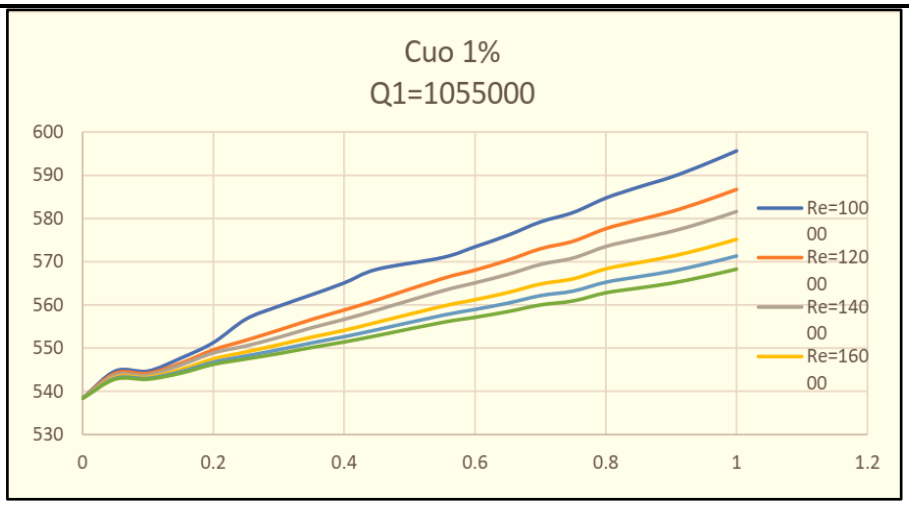


Figure (5,4): The Wall Adjacent Temperature at with Reynold number

Figure (5,5) displays graphs of the temperature of the clad wall temperature at different heat fluxes. The value for this figure is $\alpha$ =1%, and the Re value is $\alpha$ = 100000. As can be observed in Figure (5,5), as the amount of heat flow increases, so does the temperature of the clad wall.

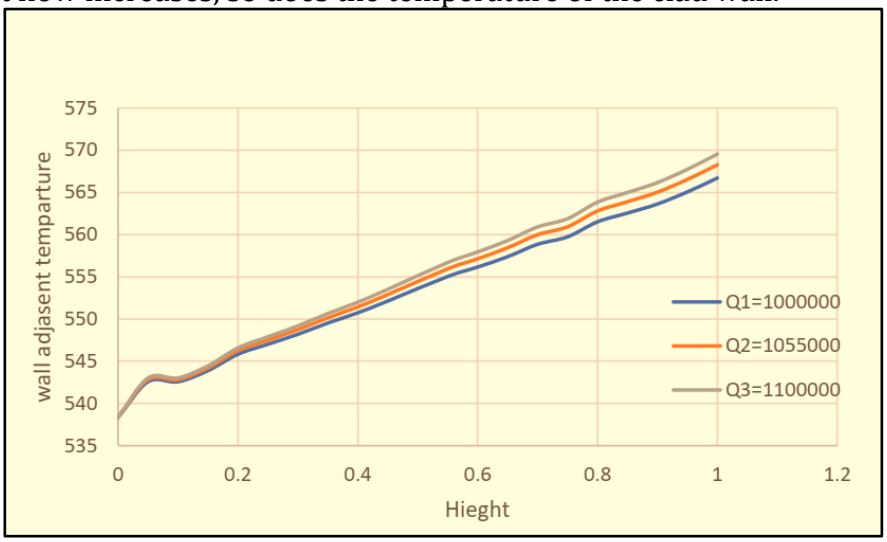


Figure (5,5): The Heat Transfer with different readings and Wall temperature on varying heat flux

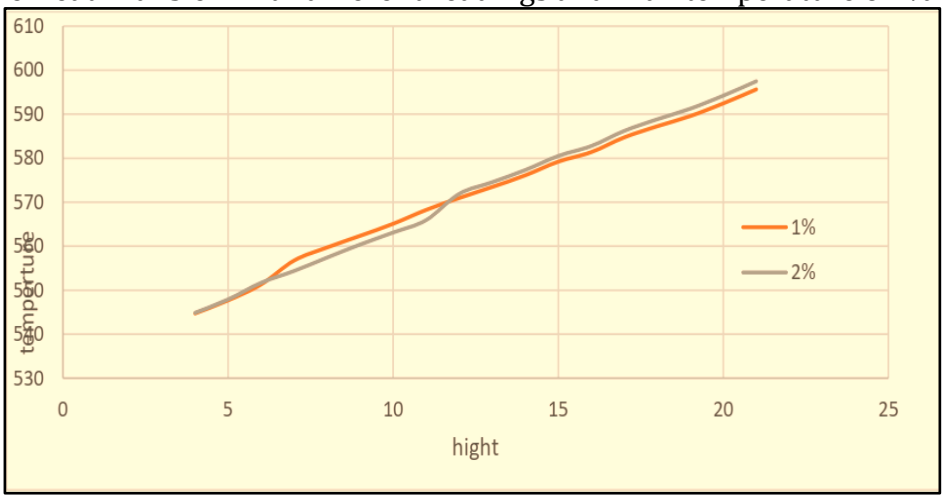


Figure (5,6): show the wall adjacent temperature with varying weight concentration .

## 6. Conclusion

This study aims to examine the impact of nanofluid characteristics on heat transfer characteristics using a numerical research. The annular hot channel Navier-Stokes equations have been used for the purpose of simulation.

The computational fluid dynamics (CFD) programme was used for doing the investigation. The present work included the influence of nanoparticles by calculating the average thermal physical parameters used in the equations governing the flow field. The simulation results indicate that the heat transfer characteristics of the CuO/water based nanofluid were improved in comparison to the base fluid, water.

This study focuses on the simulation of clad temperature and heat transport. This numerical experiment has shown the influence of nanofluid properties on heat transfer characteristics. The Navier-Stokes equations have been used for the purpose of modelling the annular hot channel. The present study used computational fluid dynamics (CFD) software. In this study, the incorporation of nanoparticles was considered by calculating the average thermophysical parameters used in the flow field equations.

The results of the simulation demonstrated that the use of CuO/water-based nanofluid led to enhanced heat transfer characteristics.Numerical experiments have shown a significant increase in heat transfer enhancement with the incorporation of CuO nanoparticles into the base fluid. The reduction in the clad wall temperature of a fuel rod is attributed to the enhanced thermal conductivity shown by the cooling nanofluid, which is directly influenced by the concentration of nanoparticles and the Reynold number of the fluid. The result in summery :

1. When compared to base fluid that is pure, the augmentation of heat transmission following the inclusion of CuO nanoparticles is substantial.
2- With an increase in particle concentration, the heat transfer coefficient increases. As an example, the local heat transfer coefficient rises by 19–24% for different Reynolds numbers and volume concentrations between 1 and 3%.
3. Due to the high thermal conductivity of cooling nanofluid, the clad wall temperature of a fuel rod is reducing while nanoparticle concentration and Reynold number are increased.
4. Heat transmission is improved since nanoparticles are smaller. As particle size decreases, the coefficient of heat transmission rises. Compared to particle sizes 20 and 30, the heat transfer value for 10 nm particles is higher.

## References


1. Acir, A., Uzun, S., Genç, Y., & Asal, Ş. (2021). Thermal analysis of the VVER-1000 reactor with thorium fuel and coolant containing al2o3, Cuo, and tio2 nanoparticles. Heat Transfer Research, 52(4), 79–93. https://doi.org/10.1615/heattransres.2021037215
2. Capson-Tojo, G., Batstone, D. J., Grassino, M., & Hülsen, T. (2022). Light attenuation in enriched purple phototrophic bacteria cultures: Implications for modelling and Reactor Design. Water Research, 219, 118572. https://doi.org/10.1016/j.watres.2022.118572
3. Elsebay, M., Elbadawy, I., Shedid, M. H., & Fatouh, M. (2016). Numerical resizing study of al2o3 and Cuo nanofluids in the flat tubes of a radiator. Applied Mathematical Modelling, 40(13–14), 6437–6450. https://doi.org/10.1016/j.apm.2016.01.039
4. Ernestová, M., Žamboch, M., Devrient, B., Roth, A., Ehrnstén, U., Föhl, J., Weissenberg, T., Gomézbriceño, D., Lapeña, J., Ritter, S., & Seifert, H. P. (2007). Crack growth behaviour of low-alloy steels for pressure boundary components under transient light water reactor operating conditions – CASTOC, part 2: Vver conditions. Corrosion Issues in Light Water Reactors, 186–199. https://doi.org/10.1533/9781845693466.3.186
5. Gupta, A., & Curtin, W. A. (2021). Analysis of the flexible boundary condition method. Modelling and Simulation in Materials Science and

Engineering, 29(8), 085002. https://doi.org/10.1088/1361-651x/ac25d3

6. Haq, R. ul, & Aman, S. (2019). Water functionalized cuo nanoparticles filled in a partially heated trapezoidal cavity with inner heated obstacle: FEM approach. International Journal of Heat and Mass Transfer, 128, 401–417. https://doi.org/10.1016/j.ijheatmasstransfer.2018.08.088
7. Hegde, R. N., Rao, S. S., & Reddy, R. (2014). Experimental investigations of pool boiling heat transfer characteristics on a vertical surface using cuo nanoparticles in distilled water. Heat Transfer Engineering, 35(14–15), 1279–1287. https://doi.org/10.1080/01457632.2013.876820
8. Janosy, J. S., Kereszturi, A., Hazi, G., Pales, J., & Vegh, E. (2010). Real-time 3D simulation of a pressurized water nuclear reactor. 2010 12th International Conference on Computer Modelling and Simulation. https://doi.org/10.1109/uksim.2010.83
9. Khan, S. U., Peng, M., Khan, S. U., Ahmad, K., & Danish, S. N. (2012). Simulation of normal/abnormal operational conditions of integral pressurized water reactor by using RELAP5/MOD3.4. International Journal of Modelling and Simulation, 32(4). https://doi.org/10.2316/journal.205.2012.4.205-5655
10. Kubo, A., Wang, J., & Umeno, Y. (2014). Development of interatomic potential for Nd–Fe–B permanent magnet and evaluation of magnetic anisotropy near the interface and grain boundary. Modelling and Simulation in Materials Science and Engineering, 22(6), 065014. https://doi.org/10.1088/0965-0393/22/6/065014
11. Reinke, N., Neu, K., & Allelein, H.-J. (2006). Astec: An integral code for simulation of severe light water reactor accidents. Volume 2: Thermal Hydraulics. https://doi.org/10.1115/icone14-89280
12. Rohini Priya, K., Suganthi, K. S., & Rajan, K. S. (2012). Transport properties of ultra-low Concentration Cuo–water nanofluids containing non-spherical nanoparticles. International Journal of Heat and Mass Transfer, 55(17–18), 4734–4743. https://doi.org/10.1016/j.ijheatmasstransfer.2012.04.035
13. Sharma, D. (2015). Numerical investigation of heat transfer characteristics in triangular channel in light water nuclear reactor by using CUO-water based nanofluids. Indian Journal of Science and Technology, 8(1), 1–6. https://doi.org/10.17485/ijst/2016/v9i16/92574
14. Sharma, D., & Pandey, K. M. (2016). Numerical investigation of heat transfer characteristics in triangular channel in light water nuclear reactor by using CUO-water based nanofluids. Indian Journal of Science and Technology, 9(16). https://doi.org/10.17485/ijst/2016/v9i16/92754
15. Sharma, D., & Pandey, K. M. (2017). Size control synthesis and characterization of zno nanoparticles and its application as zno-water based nanofluid in heat transfer enhancement in light water nuclear reactor. Kerntechnik, 82(1), 112–124. https://doi.org/10.3139/124.110635
16. Wang, P., He, J., Wei, X., & Zhao, F. (2019). Mathematical modeling of a pressurizer in a pressurized water reactor for control design. Applied Mathematical Modelling, 65, 187–206. https://doi.org/10.1016/j.apm.2018.08.006